Upper bounds on parity-violating γ-ray asymmetries in compound nuclei from polarized cold neutron capture

M. T. Gericke,[1,2,*] J. D. Bowman,[3,†] R. D. Carlini,[2] T. E. Chupp,[4] K. P. Coulter,[4,‡] M. Dabaghyan,[5] M. Dawkins,[6] D. Desai,[7,§] S. J. Freedman,[8] T. R. Gentile,[9] R. C. Gillis,[1] G. L. Greene,[7,10] F. W. Hersman,[5] T. Ino,[11] G. L. Jones,[12] M. Kandes,[4] B. Lauss,[8] M. Leuschner,[6] W. R. Lozowski,[6] R. Mahurin,[7] M. Mason,[5] Y. Masuda,[11] G. S. Mitchell,[3,‖] S. Muto,[11] H. Nann,[6] S. A. Page,[1] S. I. Penttilä,[3,†] W. D. Ramsay,[1,13] S. Santra,[6,¶] P.-N. Seo,[3,**] E. I. Sharapov,[14] T. B. Smith,[15] W. M. Snow,[6] W. S. Wilburn,[3] V. Yuan,[3] and H. Zhu[5]

(NPDGamma Collaboration)

[1]*University of Manitoba, Winnipeg, MB, Canada R3T 2N2*

[2]*Thomas Jefferson National Accelerator Facility, Newport News, Virginia 23606, USA*

[3]*Los Alamos National Laboratory, Los Alamos, New Maxico 87545, USA*

[4]*University of Michigan, Ann Arbor, Michigan 48104, USA*

[5]*University of New Hampshire, Durham, New Hampshire 03824, USA*

[6]*Indiana University, Bloomington, Indiana 47405, USA*

[7]*University of Tennessee, Knoxville, Tennessee 37996, USA*

[8]*University of California, Berkeley, California 94720-7300, USA*

[9]*National Institute of Standards and Technology, Gaithersburg, Maryland 20899-0001,USA*

[10]*Oak Ridge National Laboratory, Oak Ridge, Tennessee 37831, USA*

[11]*High Energy Accelerator Research Organization (KEK), Tukuba-shi, 305-0801, Japan*

[12]*Hamilton College, Clinton, New York 13323, USA*

[13]*TRIUMF, 4004 Wesbrook Mall, Vancouver, BC, Canada V6T 2A3*

[14]*Joint Institute for Nuclear Research, Dubna, Russia*

[15]*University of Dayton, Dayton, Ohio 45469, USA*

(Received 1 August 2006; published 19 December 2006)

Parity-odd asymmetries in the electromagnetic decays of compound nuclei can sometimes be amplified above values expected from simple dimensional estimates by the complexity of compound nuclear states. Using a statistical approach, we estimate the root-mean-square of the distribution of expected parity-odd correlations $\vec{s}_n \cdot \vec{k}_\gamma$, where $\vec{s}_n$ is the neutron spin and $\vec{k}_\gamma$ is the momentum of the γ, in the integrated γ spectrum from the capture of cold polarized neutrons on Al, Cu, and In. We present measurements of the asymmetries in these and other nuclei. Based on our calculations, large enhancements of asymmetries were not predicted for the studied nuclei and the statistical estimates are consistent with our measured upper bounds on the asymmetries.

DOI: 10.1103/PhysRevC.74.065503 PACS number(s): 11.30.Er, 25.40.Lw, 13.75.Cs, 07.85.−m

I. INTRODUCTION

One might assume that a quantitative treatment of symmetry breaking in neutron reactions with heavy nuclei would not be feasible. However, theoretical approaches exist that exploit the large number of essentially unknown coefficients in the Fock space expansion of complicated compound nuclear states in heavy nuclei to perform calculations that can be compared to experiment. If we assume that it is possible to treat the Fock space components of the states as independent random variables, one can devise statistical techniques to calculate, not the value of a particular observable, but the root-mean-square (rms) of the distribution of expected values. This strategy has been used successfully to understand certain global features of nuclear structure and reactions [1]. The distribution of neutron resonance widths, for example, have long been known to obey a Porter-Thomas distribution [2] in agreement with the predictions of random matrix theory, and statistical approaches have been used to understand isospin violation in heavy nuclei [3].

The complexity of the compound nuclear states can also amplify the size of the parity-odd asymmetries by several orders of magnitude relative to single-particle estimates. This large amplification makes it practical to use nuclear parity violation, generically expected on dimensional grounds to possess amplitudes seven orders of magnitude smaller than strong interaction amplitudes, as a new setting to investigate the validity of these statistically based theoretical approaches. Statistical analyses have successfully been applied recently to an extensive series of measurements of the parity-odd

*Corresponding author. Tel.: +1-757-269-7346 mgericke@jlab.org

†Present address: Oak Ridge National Laboratory, Oak Ridge, TN 37831, USA.

‡Present address: General Dynamics-Advanced Information Systems, 1200 Hall Drive, Ypsilanti, MI 48197, USA.

§Present address: Department of Radiation Medicine, University of Kentucky, Lexington, KY 40506, USA.

‖Present address: Department of Biomedical Engineering, University of California, Davis, CA 95616, USA.

¶Present address: Bhabha Atomic Research Center, Trombay, Mumbai 400085, India.

**Present address: Department of Physics, North Carolina State University, Raleigh, NC 27695, USA.

correlation $\vec{s}_n \cdot \vec{p}_n$ in the $A = 100$–200 mass region in neutron-nucleus scattering performed at Dubna, KEK, and Los Alamos Neutron Science Center (LANSCE) [4–7]. Although the comparison between theory and experiment in this work is still hampered somewhat by the lack of precise knowledge of the weak *NN* amplitudes and their possible modifications in the nuclear medium, theory and experiment appear to be in agreement at about the 50% level. Given the extreme complexity of the states involved, agreement between theory and experiment at this level must be counted as an overall success for the statistical approach.

Parity violation in the γ decays of nuclei is another example where statistical methods may be employed to estimate observables. In this case the observables involve the parity-odd correlation $\vec{s}_n \cdot \vec{k}_\gamma$, where $\vec{s}_n$ is the neutron spin and $\vec{k}_\gamma$ is the momentum of the γ photon [6–8]. Just as for neutron scattering, neutron capture on elements with a large number of nucleons produces compound nuclei in highly excited states. These nuclei exhibit a huge ($> 10^6$) number of possible state configurations with different angular momenta and parity, and the number of transitions with different amplitudes that the compound nucleus may make to its ground state is correspondingly large as well. Because of the large number of energy levels in the compound nucleus, formed by neutron capture, one may hope that the calculation of the mean-square matrix elements for the transition amplitudes may also amount to a summation of a large number of uncorrelated random contributions as in the case of the total cross section. One can then use statistical arguments to estimate the rms value of the parity-odd γ-ray asymmetry.

However, the case of parity violation in (n,γ) reactions in heavy nuclei is not quite as simple as parity violation in the total cross section for both theoretical and experimental reasons. For the total cross section, the amplification of parity violation effects is dominated by the mixing amplitude of the weak interaction, between two compound nuclear states of opposite parity (in practice S-wave and P-wave compound states). Because the total cross section is proportional to the forward elastic scattering amplitude, by the optical theorem, there is only one such contribution for any pair of opposite parity compound states. For inelastic processes such as the (n,γ) reaction, however, the weak mixing between compound states can occur in either the initial or final nuclear states, and because these states are distinct in an inelastic reaction there are two possible sources of compound nuclear amplification of the parity-odd effect rather than one [7]. Because of the large density of states in the initial state near neutron separation energy, the initial state mixing will involve a larger number of components in the wave function for γ transitions to low-lying states and therefore lead to a larger amplification. However, one also has contributions from transitions to higher-lying states where final-state mixing is somewhat more important. Experimentally, precise measurements of parity-odd asymmetries are more practical for the total integrated γ spectrum rather than individual γ transitions. But a calculation of the asymmetry of the integral γ spectrum requires an additional averaging over the large number of distinct final states. In addition the integral measurement also senses γ cascades in addition to single transitions. Parity-odd correlations in the integrated γ spectra of ^{35}Cl, ^{81}Br, ^{113}Cd, ^{117}Sn, and ^{139}La have previously been calculated by Flambaum and Sushkov [6] and by Bunakov *et al.* [9]. However, more experimental information on parity-odd asymmetries in integral γ spectra from heavy nuclei are needed in any attempt to make progress in this area.

We have searched for parity-odd directional γ-ray asymmetries in the capture of cold polarized neutrons on ^{27}Al, Cu, and ^{115}In at LANSCE. We have performed a simple statistical estimate of the mean-square value for the parity-odd asymmetries in these nuclei and obtain expected upper bounds that are consistent with experiment. In addition, we performed measurements of the directional γ-ray asymmetry for polarized cold neutron capture on ^{35}Cl and on ^{10}B. ^{35}Cl is known to possess a large parity-odd γ asymmetry [10,11] and it is used to verify the sensitivity of our apparatus. ^{10}B is used extensively throughout the experiment for neutron shielding. Searches for parity-odd γ asymmetries on several other nuclei (^{45}Sc, ^{51}V, ^{59}Co, ^{48}Ti, ^{55}Mn) are in progress.

The motivation for further measurements in the mass region $30 < A < 100$ is that these additional measurements may make it possible to improve our knowledge of the weak spreading width using statistical methods similar to those developed by the TRIPLE collaboration [5]. The TRIPLE collaboration measured many parity-violating asymmetries in the helicity dependence in compound-nuclear total cross sections. They extracted the weak spreading width for the mass region around 100 and 240 using a likelihood approach. We show in equation Eq. (11), below, that the average parity-violating asymmetry in capture γs is a product of the parity-violating admixture in the capture state, ϵ, and a Gaussian random variable $\mathcal{B}_\gamma$. We calculate the rms width of the Gaussian random variable. Bowman *et al.* [12] give the distribution of ϵ in situations involving different degrees of *a priori* knowledge of spectroscopic information. The present work allows the construction of the likelihood function for the weak spreading width from data on parity violation in capture γs.

The measurements in this article are being conducted in preparation for an experiment to search for the parity-violating γ-ray asymmetry in the capture of polarized neutrons on protons by the NPDGamma collaboration. The apparatus constructed for the NPDGamma experiment is capable of measuring γ-ray asymmetries with an accuracy of 10^{-8}. The motivation for choosing the above targets is that they are components of the NPDGamma apparatus. Neutrons form the beam and scattered neutrons capture on these components. We therefore needed to measure their γ asymmetries to control potential systematic errors.

The remainder of the article is organized as follows. We first provide a brief theory section in which we outline the calculation and estimate the expected rms of the γ-ray asymmetry in a current mode γ-ray detector from the nuclei used in the experiment. We give a short overview of the experimental layout and then describe the measurements. We conclude with a discussion on the results and the associated implications.

II. THEORY AND STATISTICAL ESTIMATES

The simplest nuclear reaction that can produce a parity-odd directional distribution of γ rays is the capture of polarized neutrons on protons. The differential cross section in this simple system can be calculated explicitly from the transition amplitudes of the electro-magnetic part of the Hamiltonian between initial (capture) and final (bound) two-nucleon states, which possess mixed parity due to the NN weak interaction. In the $\vec{n} + p \to d + \gamma$ reaction the primary process is the strong interaction induced parity conserving $M1$ transition between the singlet and triplet S-wave states $^1S_0$, $^3S_1$.The weak interaction introduces a small parity non-conserving admixture of P-wave states in the initial singlet and the final triplet S-wave states. The largest contribution to the hadronic weak interaction comes from pion exchange and the measurement of the parity violating up-down asymmetry, A_γ, in the angular distribution of 2.2-MeV γ rays with respect to the neutron spin direction

$$\frac{d\sigma}{d\Omega} \propto \frac{1}{4\pi}(1 + A_\gamma \cos\theta), \tag{1}$$

almost completely isolates the term proportional to the weak pion-nucleon coupling constant f_π^1 [13]. Here $\cos\theta$ is the angle between the neutron spin direction and the γ-ray momentum.

For the $\vec{n} + p \to d + \gamma$ reaction, it can be shown that there is a simple expression for the γ-ray asymmetry in terms of the matrix elements between initial and final states

$$A_\gamma \propto \mathrm{Re}\,\frac{\epsilon\langle {}^3P_1|\mathbf{E1}|{}^3S_1\rangle}{\langle {}^3S_1|\mathbf{M1}|{}^1S_0\rangle}. \tag{2}$$

Here

$$\epsilon = \frac{\langle\psi_{\alpha'}|W|\psi_\alpha\rangle}{\Delta E} \tag{3}$$

and $\alpha = \{J, L, S, p\}$ (p = parity).

In heavy nuclei the interference term that produces the asymmetry is much more complicated, involving many states. Here, a neutron may capture into an S- or P-wave state close to the neutron separation energy (S_n) and the weak interaction mixes the corresponding amplitudes perturbatively. For almost all nuclei except in few-body systems it is essentially impossible to calculate the parity-violating asymmetry from the strong and weak Hamiltonian, because of the large number of γ-ray transitions. However, because of the large number of possible electromagnetic transitions in the compound nucleus, the calculation of the mean-square matrix elements for the transition amplitudes amounts to a summation of a large number of uncorrelated random amplitudes that are approximately independent of the transition energy for $E \leqslant S_n$. One can then hope to use statistical arguments to estimate the rms value of the asymmetry from nuclei close to a certain neutron separation energy.

Due to the large density of states close to the neutron separation energy and the correspondingly small level spacing $D \simeq \Delta E_c$, parity violation is expected to be dominated by the mixing of the two closest S- and P-wave states near S_n, in the initial or capture state, and it is expected on general grounds that parity violation due to mixing with lower-lying states may be neglected. The parity-violating asymmetry comes from interference between $E1$ and $M1$ γ transitions. The γ-ray asymmetry from the decaying compound nucleus as measured in a current-mode γ detector is given by

$$A_\gamma = \epsilon\mathcal{B}_\gamma. \tag{4}$$

Where

$$\mathcal{B}_\gamma = \xi \cdot F(J_T, J_i) \times \frac{2\,\mathrm{Re}\left[\sum_{J_f}\langle J_f^p|\mathbf{E1}|J_i^{p'}\rangle\langle J_i^p|\mathbf{M1}|J_f^p\rangle E_{\gamma,if}^4\right]}{\sum_{J_f}\left(\left|\langle J_f^p|\mathbf{M1}|J_i^p\rangle\right|^2 + \left|\langle J_f^p|\mathbf{E1}|J_i^{p'}\rangle\right|^2\right)E_{\gamma,if}^4} \tag{5}$$

characterizes the γ cascade and, with the numerator being a sum of independent random variables, will have a Gaussian distribution, according to the central-limit theorem. Here the transitions are between initial (i) and final (f) compound nuclear states with total angular momentum (J_i, J_f) and parity (p, p'). $F(J_T, J_i)$ is the angular-momentum coupling factor resulting from the compound state polarization [6]

$$F(J_T, J_i) = (-1)^{2J_i+1/2+J_T}3(2J_i+1)\begin{Bmatrix} 1 & 1/2 & 1/2 \\ J_T & J_i & J_i \end{Bmatrix},$$

where J_T is the angular momentum of the target nucleus before neutron capture.

The dependence on the γ-ray transition energy E_γ in Eq. (5) comes from the phase-space factor ($E_\gamma^{3/2}$) in the transition amplitude and the linearity ($\propto E_\gamma$) of the detector response as a function of energy in a current mode γ detector. The factor

$$\xi = \frac{\sum_f I_{\gamma,if}E_{\gamma,if}}{S_n} \Rightarrow \frac{1}{S_n}\frac{\int_0^{S_n}E_\gamma^4\rho_f(E_\gamma)dE_\gamma}{\int_0^{S_n}E_\gamma^3\rho_f(E_\gamma)dE_\gamma}$$

arises because the current mode γ detector possesses no energy resolution and therefore sees a superposition of currents from all transitions. This has the effect of diluting the asymmetry ($0 < \xi \leqslant 1$). Here,

$$I_{\gamma,if} = \frac{\left(\left|\langle J_f^p|\mathbf{M1}|J_i^p\rangle\right|^2 + \left|\langle J_f^p|\mathbf{E1}|J_i^{p'}\rangle\right|^2\right)E_{\gamma,if}^3}{\sum_{J_f}\left(\left|\langle J_f^p|\mathbf{M1}|J_i^p\rangle\right|^2 + \left|\langle J_f^p|\mathbf{E1}|J_i^{p'}\rangle\right|^2\right)E_{\gamma,if}^3}$$

is the relative intensity of a given transition.

We estimate the density of final states using the back-shifted Fermi gas model (BSFGM) as [14,15],

$$\rho_f(E_x) = \sum_J \frac{2J+1}{24\sqrt{2}\sigma^3 a^{1/4}} \times \frac{\exp[2\sqrt{a(E_x-\Delta)} - J(J+1)/2\sigma^2]}{(E_x-\Delta+t)^{5/4}}, \tag{6}$$

where J is summed over $J_f - 1$, J_f, $J_f + 1$ for each final compound nuclear state. Here, a [MeV^{-1}] and Δ [MeV] are determined from experimental data and the temperature parameter t is defined by $E_x - \Delta = at^2 - t$. $\sigma^2 = I_{\mathrm{eff}}t/\hbar^2 \simeq 0.015A^{5/3}t$ is the spin cut-off parameter and the *effective* moment of inertia I_{eff} takes on values between 50 and 100% of the rigid-body moment of inertia $I_{\mathrm{rig}} = \frac{2}{5}MR^2$. The level density Eq. (6) is derived assuming random coupling of angular momenta and the spin cut-off parameter arises as a result of this treatment [15]. The excitation energy $E_x = S_n - E_\gamma$ is

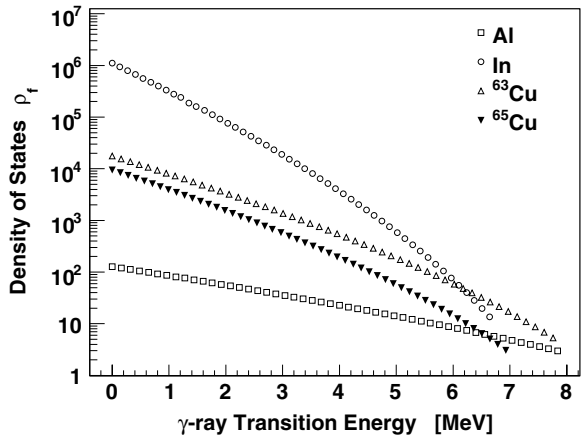

FIG. 1. Density of final states in the excited compound nuclei investigated in this work as a function of γ-ray transition energy up to the neutron separation energy. There are many more states at low γ energies than at high energies, and the decaying nucleus emits many low-energy γ rays before reaching the ground state. The level density is calculated according to the back-shifted Fermi gas model.

the energy of the nucleus after the γ-ray transition from the capture state. E_x may be zero if the transition is to the ground state. Figure 1 shows the predicted density of final states, using this model, for the ^{27}Al , Cu, and ^{115}In, nuclei as a function of γ-ray energy.

For comparison and to estimate the uncertainty in the calculated asymmetries due to the model we also determine the asymmetries using a constant temperature model (CTM) of the final density of states [14]

$$\rho_f(E_x) = \frac{1}{T}\exp\left(E_x - \Delta\right)/T. \tag{7}$$

The aim of this calculation is to find a simple "generic" formula that holds for many nuclei and provides a good estimate of the size of an asymmetry one can expect in a measurement of this nature. The denominator in Eq. (5) is the parity-allowed transition from the initial compound state (J_i) after capture of an S-wave neutron. This transition has the largest amplitude and basically determines the intensity of the γ signal. In general $E1$ transitions outnumber $M1$ transitions and the denominator is primarily $E1$ for most nuclei. We point out, though, that if one has initial states such that all or most parity-allowed transitions are $M1$ in the range of expected γ-ray energies, as determined by the density of states (as is the case for Al and In), then the denominator would be $M1$.

The rms of the γ-ray asymmetry can then be estimated as follows. We use the electric and magnetic dipole transition rates that are given by

$$\begin{aligned}\Gamma_{E1} &= 2\pi\left\langle\left|\left\langle J_f^{p'}\left|\mathbf{E1}\right|J_i^{p}\right\rangle\right|^2\right\rangle\rho_f(S_n),\\ \Gamma_{M1} &= 2\pi\left\langle\left|\left\langle J_f^{p}\left|\mathbf{M1}\right|J_i^{p}\right\rangle\right|^2\right\rangle\rho_f(S_n),\end{aligned} \tag{8}$$

respectively. The transition rates are strength functions. As the density of states increases, the average matrix element squared decreases and the transition rates are constant or slowly varying functions of energy.

The rms of the detected intensity of the γ rays that depopulate the initial state is given by taking the average of the squared denominator in Eq. (5). Then, invoking the randomness in the transition amplitudes (under the assumption that the correlation is zero, so that the cross terms vanish), we find

$$\begin{aligned}&\left\langle\left(\sum_{J_f}\left(\left|\left\langle J_f^{p'}\left|\mathbf{E1}\right|J_i^{p}\right\rangle\right|^2 + \left|\left\langle J_f^{p}\left|\mathbf{M1}\right|J_i^{p}\right\rangle\right|^2\right)E_{\gamma,if}^4\right)^2\right\rangle\\ &\quad\simeq\left(\sum_{J_f}\left\langle\left|\left\langle J_f^{p'}\left|\mathbf{E1}\right|J_i^{p}\right\rangle\right|^2\right\rangle E_{\gamma,if}^4\right)^2\\ &\qquad+\left(\sum_{J_f}\left\langle\left|\left\langle J_f^{p}\left|\mathbf{M1}\right|J_i^{p}\right\rangle\right|^2\right\rangle E_{\gamma,if}^4\right)^2\\ &\quad=\left[\int_0^{S_n}E_\gamma^4\frac{\Gamma_{E1}}{2\pi\rho_f(S_n)}\rho_f(S_n)dE_\gamma\right]^2\\ &\qquad+\left[\int_0^{S_n}E_\gamma^4\frac{\Gamma_{M1}}{2\pi\rho_f(S_n)}\rho_f(E_\gamma)dE_\gamma\right]^2\\ &\quad=\frac{\Gamma_{E1}^2+\Gamma_{M1}^2}{4\pi^2\rho_f^2(S_n)}\left[\int_0^{S_n}E_\gamma^4\rho_f(E_\gamma)dE_\gamma\right]^2.\end{aligned} \tag{9}$$

The factor $\rho_f(E_\gamma)dE_\gamma$ arises in the standard fashion, when converting the sum over final states into an integral.

The rms of the interference term in the numerator gives

$$\begin{aligned}&4\left\langle\left(\sum_{J_f}\left\langle J_f^{p'}\left|\mathbf{E1}\right|J_i^{p}\right\rangle\left\langle J_i^{p}\left|\mathbf{M1}\right|J_f^{p}\right\rangle E_{\gamma,\mathrm{if}}^4\right)^2\right\rangle\\ &\quad\simeq 4\sum_{J_f}\left\langle\left|\left\langle J_f^{p'}\left|\mathbf{E1}\right|J_i^{p}\right\rangle\right|^2\right\rangle\left\langle\left|\left\langle J_i^{p}\left|\mathbf{M1}\right|J_f^{p}\right\rangle\right|^2\right\rangle E_{\gamma,if}^8\\ &\quad=4\int_0^{S_n}E_\gamma^8\frac{\Gamma_{E1}}{2\pi\rho_f(S_n)}\frac{\Gamma_{M1}}{2\pi\rho_f(S_n)}\rho_f(E_\gamma)dE_\gamma\\ &\quad=\frac{\Gamma_{E1}\Gamma_{M1}}{\pi^2\rho_f^2(S_n)}\int_0^{S_n}E_\gamma^8\rho_f(E_\gamma)dE_\gamma,\end{aligned} \tag{10}$$

where we again used the randomness in the transition amplitudes in going to the second line. With this, the rms asymmetry can be estimated for each target from

$$\sqrt{\left\langle A_\gamma^2\right\rangle} \simeq \epsilon\sigma_{B_\gamma}. \tag{11}$$

Where

$$\sigma_{B_\gamma} = 2F(J_T, J_i)\xi\sqrt{\frac{\Gamma_{E1}\Gamma_{M1}}{\Gamma_{E1}^2+\Gamma_{M1}^2}\frac{\int_0^{S_n}E_\gamma^8\rho_f(E_\gamma)dE_\gamma}{\left(\int_0^{S_n}E_\gamma^4\rho_f(E_\gamma)dE_\gamma\right)^2}}. \tag{12}$$

To calculate the rms asymmetry for a particular nucleus, one must then determine whether the transitions to the ground state are mostly $E1$ or $M1$ and omit the corresponding amplitude in the denominator. In the case of ^{27}Al and ^{115}In we then have Γ_{M1}/Γ_{E1}, whereas for Cu we have Γ_{E1}/Γ_{M1}.

TABLE I. rms γ-*ray* asymmetry values and associated variables, as estimated from the statistical approach ($I \equiv \int_0^{S_n} dE_\gamma E_\gamma^8 \rho(E_\gamma)/(\int_0^{S_n} dE_\gamma E_\gamma^4 \rho(E_\gamma))^2, D \equiv D_o \sum 2J_i + 1) D_o$ was taken from [19,20].

Calculated rms γ-*ray* Asymmetries (BSFGM)									
	S_n[MeV]	J_T	J_i	$F(J_T, J_i)$	D[eV]	ξ^2	ϵ^2	I	$\sqrt{\langle A_\gamma^2 \rangle}$
^{27}Al	8.0	5/2	2, 3	0.3	1.2×10^5	0.6	2.4×10^{-13}	6.5×10^{-2}	1.3×10^{-7}
^{63}Cu	7.9	3/2	1, 2	-0.4	4.8×10^3	0.5	6.0×10^{-12}	1.6×10^{-3}	1.4×10^{-8}
^{65}Cu	7.1	3/2	1, 2	-0.4	8.0×10^3	0.5	3.6×10^{-12}	2.7×10^{-3}	1.4×10^{-8}
^{115}In	6.8	9/2	4, 5	0.4	400	0.4	7.2×10^{-11}	7.3×10^{-5}	7.5×10^{-8}
Calculated rms γ-*ray* Asymmetries (CTM)									
	S_n[MeV]	J_T	J_i	$F(J_T, J_i)$	D[eV]	ξ^2	ϵ^2	I	$\sqrt{\langle A_\gamma^2 \rangle}$
^{27}Al	8.0	5/2	2, 3	0.3	1.2×10^5	0.7	2.4×10^{-13}	5.0×10^{-2}	1.3×10^{-7}
^{63}Cu	7.9	3/2	1, 2	-0.4	4.8×10^3	0.6	6.0×10^{-12}	2.5×10^{-3}	1.8×10^{-8}
^{65}Cu	7.1	3/2	1, 2	-0.4	8.0×10^3	0.6	3.6×10^{-12}	3.7×10^{-3}	1.7×10^{-8}
^{115}In	6.8	9/2	4, 5	0.4	400	0.4	7.2×10^{-11}	9.9×10^{-5}	8.8×10^{-8}

Substituting the experimental value of the hadronic weak spreading width ($\Gamma_W = 1.8^{+0.4}_{-0.3} \times 10^{-7}$ eV) [5] and using

$$\epsilon^2 = \frac{\Gamma_W}{2\pi\rho_i}\frac{1}{D^2} \simeq \frac{\Gamma_W}{2\pi D}$$

together with the fact that $E1$ transitions are approximately 10 times faster than $M1$ transitions, $\Gamma_{E1} \simeq 10\Gamma_{M1}$ [16,17], the rms asymmetry can be calculated for different nuclei and neutron separation energies. When evaluating Eq. (11) for aluminum, for example, the single-particle level spacing is approximately $D \simeq 120$ keV, the dilution factor $\xi^2 \simeq 0.6$, and the ratio of integrals in Eq. (11) can be numerically evaluated to give $\simeq 6.5 \times 10^{-2}$. The expected rms value of the γ asymmetry is then about 1.3×10^{-7}. The rms γ-ray asymmetry values and other associated variables for the nuclei studied in this work are listed in Table I.

A. Theory discussion

The results in Tables I and IV show no large enhancements. There are several reasons why one may expect this behavior. For example, the levels are highly degenerate, the sign of the asymmetry is random, and the transitions mix incoherently, producing a $1/\sqrt{N}$ suppression. There is also no kR enhancement for the direct capture calculations done here, which are appropriate for the low neutron energies used in these experiments.

In Ref. [6] Flambaum and Sushkov calculated the average value for the integral γ-ray spectrum relative to the S-wave amplitude for thermal neutrons,

$$a_o = \frac{g}{4k^2}\frac{T_s^2 \Gamma_{\rm eff}^{(\gamma)}}{(E - E_s)^2 + \frac{1}{4}\Gamma_s^2},$$

which is far from P-wave resonance so that its contribution to the cross section can be neglected. The rms asymmetry is given, in their notation, by

$$\langle A_9 \rangle = -2\,\mathrm{Re}\left(\frac{\epsilon}{E - E_p - \frac{1}{2}i\Gamma_p}\right)\frac{F(J_T, J_i)}{3\sqrt{2J_i + 1}}(r). \tag{13}$$

Where r is an integral over the $E1$ and $M1$ radiative strength functions, detection efficiency, and density of final states, corresponding to our integral in Eq. (10). Equation (13) may be compared to our result above. Flambaum and Sushkov also state that the γ-ray asymmetry arises as a result of the *E1-M1* interference, that the transitions are random, and that the asymmetry is statistically suppressed after averaging.

The main difference between our calculations and those done by Flambaum and Sushkov is that they consider a P-wave resonance near the thermal (or cold) region mixed by parity violation with one S-wave resonance, whereas our treatment takes account of all S- and P-wave resonances, but in the tail, far from resonance, at the average spacing D or more.

III. EXPERIMENT

The NPDGamma apparatus used for the measurements is located on flight path 12 at the Manuel Lujan Jr. Neutron Scattering Center at LANSCE. The LANSCE linear accelerator delivers 800-MeV protons to a storage ring, which compresses the beam to 250-ns-wide pulses at the base. The protons from the storage ring are incident on a split tungsten target at a rate of 20 Hz and the resulting spallation neutrons are cooled by and backscattered from a cold H_2 moderator with a surface area of 12×12 cm^2. For the measurements described here, the cold neutrons were transported to the experimental apparatus by a neutron guide and then transversely polarized by transmission through a polarized ^{3}He cell. Three ^{3}He ion chambers were used to monitor beam intensity and polarization. A radio frequency spin flipper was used to reverse the neutron spin direction on a pulse-by-pulse basis. The polarized neutrons then captured on a target placed in the center of the γ detector array. The γ rays from the neutron capture were detected

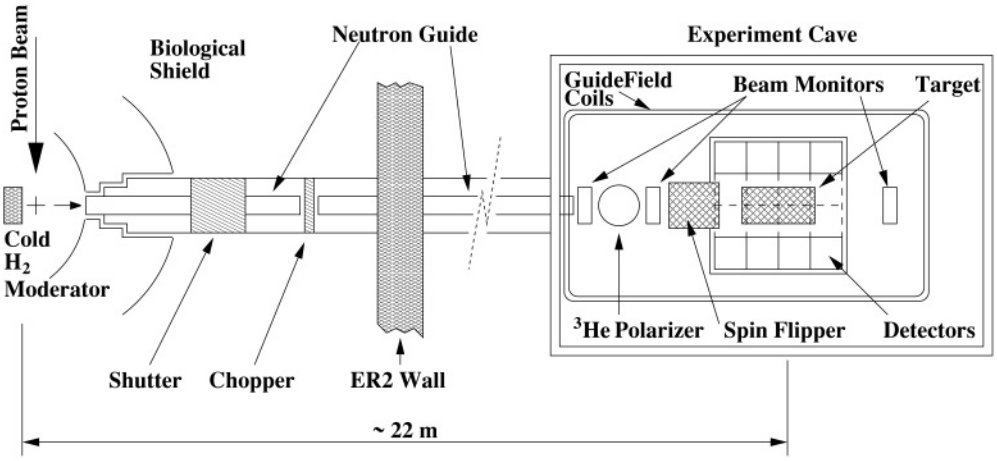

FIG. 2. Schematic of the experimental setup.

by an array of 48 CsI(Tl) detectors operated in current mode [20,21]. The entire apparatus was in a homogeneous 10-G field, which was required to maintain the neutron spin downstream of the polarizer, with a gradient of less than 1 mG/cm to make spin-dependent Stern-Gerlach steering of the polarized neutron beam negligible.

Figure 2 shows the flight path and experimental setup. The distance between the moderator and target is about 22 m. The flight path 12 beam line consists of a neutron guide, a shutter, and a beam chopper. The pulsed spallation neutron source allowed us to know the neutron time of flight or energy accurately. The chopper is used to define the time of flight frame and to prevent neutrons from different frames from mixing and thus diluting the neutron energy information. In this experiment the chopper was used to close the beam line before the end of the frame, which allowed us to take beam-off (pedestal) data for $\simeq$6 ms at the end of each neutron pulse that is needed for detector pedestal and background studies (Fig. 3). The last 10 ms after sampling stops is used by the DAQ for data transfer. A detailed description of the FP12 neutron guide and performance is given in Ref. [22]. The measured moderator brightness has a maximum of 1.25×10^8 n/(s $\cdot$ cm^2 $\cdot$ sr $\cdot$ meV $\cdot$ μA) for neutrons with an energy of 3.3 meV.

The neutrons were polarized by passing through a 12-cm-diameter glass cell containing polarized ^{3}He ([23,24] and references within). The beam polarization was measured with the beam monitors using neutron transmission. (The ^{3}He polarization can be monitored using nuclear magnetic resonance). For γ-asymmetry measurements, the figure of merit is the statistical accuracy that can be reached for a certain running time, which is proportional to the product $P_n\sqrt{T_n}$, where T_n is the neutron transmission through the cell and P_n is the neutron polarization [25]. The neutron transmission increases with energy, whereas the neutron polarization decreases with energy. In the analysis of the data the neutron polarization was calculated separately for each run by fitting the transmission spectrum to the expression $P_n = \tanh(\sigma_c nl P_{\mathrm{He}})$, using a ^{3}He thickness of 4.84 bar $\cdot$ cm, which was separately measured. Here, $\sigma_c = \sigma_o/\sqrt{E}$ with neutron energy E in units of meV, and $\sigma_o = 27168$ b, $nl = 4.84 \cdot 2.688 \times 10^{23}$ atoms/m^2.

The primary technique for reducing false asymmetries generated by gain nonuniformities, slow efficiency changes and beam fluctuations is frequent neutron spin reversal. This allows asymmetry measurements to be made in each spin state for opposing pairs of detectors and for consecutive pulses with different spin states, thereby suppressing the sensitivity of the measured asymmetry to detector gain differences, drifts, and intensity fluctuations. By carefully choosing the sequence of spin reversal, the linear and quadratic components of time-dependent detector gain drifts in a sequence can be greatly suppressed. To achieve the neutron spin reversal, the experiment employed a radio frequency adiabatic neutron spin rotator (RFSR) [26] that operates at 29 kHz for the 10-G guide field. The neutron spin direction is reversed when the RFSR is on and is unaffected when it is off. The spin flip efficiency averaged over the beam cross section (5 cm diameter) was measured to be about 99%.

The polarized neutrons then captured on a target placed in the center of the γ detector array. The targets were thick enough to stop most of the neutron beam by capture or scattering with diameters larger than the beam cross section. The capture γ

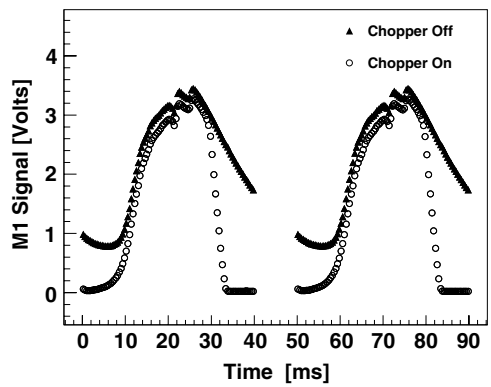

FIG. 3. Normalized signal from the first beam monitor downstream of the guide exit. The solid triangles show the signal obtained from a run where the chopper was parked open. The open circles correspond to a run taken with the chopper running.

TABLE II. Targets with their relative background contributions (target in versus target out). In each case the maximum value is stated for the detector with the largest background signal. The relative amount of background varies, because the magnitude of the γ-ray signal varies with target, whereas the target-out background remains constant.

Relative background		
B_4C	$\leqslant$	17%
Al	$\leqslant$	15%
In	$\leqslant$	11%
CCl_4	$\leqslant$	8%
Cu	$\leqslant$	7%

signals from all of the targets measured were large compared to noise and background.

The housing for the 33-cm^3 liquid CCl_4 target was made of Teflon. The CCl_4 liquid is 99.9% chemically pure, with less than 0.01% water content. The aluminum and copper targets consisted of a number of sheets supported by an aluminum frame. Each target sheet is a square with 8.5-cm sides and of $\sim$1 mm in thickness. The arrangement of the target into sheets with a gap between the sheets reduced γ attenuation in the target. The total length of the target (including gaps) was 30 cm. Target-out background runs and runs with the empty frame were conducted as well, and the background is taken into account in the final determination of the asymmetry (see Table II). The boron target consists of a 1-cm-thick, 15 $\times$ 15 cm sheet of sintered B_4C glued to an aluminum holder consisting of a simple (thin) aluminum sheet. The indium target was approximately 12 mm thick, covering a circular cross-sectional area with a radius of $\sim$3 cm at the center of the beam. For each of the targets the beam was collimated to a diameter of about 5 cm.

The depolarization of neutrons *via* spin flip scattering from the nuclei dilutes the asymmetry. For all targets the neutron depolarization is a small effect that can be estimated to sufficient accuracy for nonmagnetic materials using the known neutron coherent and incoherent cross sections. Table III lists the estimated spin-flip probabilities for the targets used and the corresponding calculated average correction factors $\langle \Delta_{\rm dep}(t_i) \rangle$. The degree of spin flip scattering is neutron energy dependent and a Monte Carlo calculation for the depolarization as a function of neutron energy was applied to the data.

TABLE III. Spin-flip probability estimate and corresponding corrections to the asymmetry due to depolarization in the target region.

Neutron depolarization		
	$2\sigma_{\rm inc}/3\sigma_{\rm tot}$	$\langle \Delta_{\rm dep}(t_i) \rangle$
Al	3×10^{-3}	1
Cu	2×10^{-2}	0.95
CCl_4	7×10^{-2}	0.95
In	2×10^{-3}	1
B_4C	5×10^{-4}	1

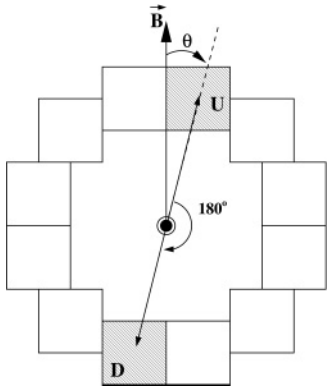

FIG. 4. A ring of detectors and one up-down pair, as seen with beam direction into the page. $\vec{B}$ is the magnetic holding field defining the direction of the neutron polarization.

The detector array consists of 48 CsI(Tl) cubes arranged in a cylindrical pattern in 4 rings of 12 detectors each around the target area (Fig. 4). In addition to the conditions set on the detector array by the need to preserve statistical accuracy and suppress systematic effects, the array was also designed to satisfy criteria of sufficient spatial and angular resolution, high efficiency, and large solid angle coverage [20]. Because of the possible small size of the asymmetries and the proposed measurement accuracy the average rate of neutron capture and the corresponding γ rate in the detectors must be high to keep the run-time reasonable. Because of the high rates and for a number of other reasons discussed in Ref. [20], the detector array uses current mode γ detection. Current mode detection is performed by converting the scintillation light from CsI(Tl) detectors to current signals using vacuum photo diodes (VPD), and the photocurrents are converted to voltages and amplified by low-noise solid-state electronics [21].

In current mode detection, the counting statistics resolution is limited by the rms width in the sample distribution. For our detector array this width is dominated by fluctuations in the number of electrons produced at the photocathode of the VPD, which is dominated by γ-ray counting statistics when the beam is on. During beam on measurements, the shot noise rms width is then given by [27]

$$\sigma_{I_{\rm shot}} = \sqrt{2qI}\sqrt{f_B}, \tag{14}$$

where q is the amount of charge created by the photo cathode per detected γ-ray, I is the average photocurrent per detector, and f_B is the sampling bandwidth, set by the 0.4-ms time bin width in the time of flight spectrum [20,28].

IV. ANALYSIS AND RESULTS

A. Asymmetry definition

For a point target and a detector array with perfect spatial resolution, the measured γ-ray angular distribution would

be proportional to the differential cross-section $Y = 1 + A_\gamma \cos\theta$, where θ is the angle between the neutron polarization and the momentum of the emitted photon and $A_{\gamma,UD}$ is the parity-odd up-down (UD) asymmetry. A third term is present if a parity-conserving (PC) left-right (LR) asymmetry exists [29]. In that case $Y = 1 + A_{\gamma,UD}\cos\theta + A_{\gamma,LR}\sin\theta$. However, the relationship between the basic expression for the γ-ray yield and the measured asymmetry is complicated by a number of small neutron energy-dependent effects. A separate asymmetry is calculated for each detector pair, as defined in Fig. 4.

The physics asymmetry for a given detector pair p, spin sequence j, and neutron time of flight t_i is given by

$$\begin{aligned}&\left[A_{UD}^{j,p}(t_i) + \beta A_{UD,b}^{j,p}(t_i)\right]\langle G_{UD}(t_i)\rangle \\ &\quad + \left[A_{LR}^{j,p}(t_i) + \beta A_{LR,b}^{j,p}(t_i)\right]\langle G_{LR}(t_i)\rangle \\ &= \frac{\left[A_{\rm raw}^{j,p}(t_i) - A_g^p A_f(t_i) - A_{\rm noise}^p\right]}{P_n(t_i)\Delta_{\rm dep}(t_i)\Delta_{sf}(t_i)}\end{aligned} \tag{15}$$

Here, $A_{\rm raw}^{j,p}(t_i)$ is the measured asymmetry. The background asymmetries ($A_{UD,b}^{j,p}$, $A_{LR,b}^{j,p}$) and the relative signal level (β) must be measured in auxiliary measurements. A_g^p is the gain asymmetry between the detector pair and $A_f(t_i)$ is the asymmetry from pulse to pulse beam fluctuations. The neutron energy and detection efficiency weighted spatial average detector cosine (up-down asymmetry) with respect to the (vertical) neutron polarization is given by $\langle G_{UD}(t_i)\rangle \simeq \cos\theta$, whereas the detector sine (left-right asymmetry) is given by $\langle G_{LR}(t_i)\rangle \simeq \sin\theta$. These detector-target geometry corrections have been modeled for each target geometry. Also included are the correction factors due to the neutron beam polarization $[P_n(t_i)]$, the spin flip efficiency $[\Delta_{sf}(t_i)]$, and the neutron depolarization in the target $[\Delta_{\rm dep}(t_i)]$.

The measured asymmetry ($A_{\rm raw}^{j,p}$) for each detector pair and neutron energy can be extracted in the usual way, by forming a ratio of differences between cross sections to their sum. However, to suppress first- and second-order detector gain drifts [30] the raw asymmetries were formed for all valid sequences of eight macro pulses with the correct neutron spin state pattern

$$A_{\rm raw}^{j,p}(t_i) = \frac{\sum_{s=\uparrow}[U_s(t_i) - D_s(t_i)] - \sum_{s=\downarrow}[U_s(t_i) - D_s(t_i)]}{\sum_{s=\uparrow}[U_s(t_i) + D_s(t_i)] + \sum_{s=\downarrow}[U_s(t_i) + D_s(t_i)]}. \tag{16}$$

Here the sum is over all four signals with the corresponding spin state in a spin sequence for the up (U) and down (D) detector in a pair. A so-called valid eight-step sequence of spin states is defined as ($\uparrow\downarrow\downarrow\uparrow\downarrow\uparrow\uparrow\downarrow$). Asymmetries were measured for 55 different neutron energies between approximately 2 and 16 meV, with a resolution of ~0.2 to 1.0 meV per time bin, respectively.

It is important to realize that signal fluctuations that are not correlated with the switching of the neutron polarization direction, such as beam and detector gain fluctuations, will average out and do not contribute to the asymmetry. It is, however, essential that these signals have an rms width that is small compared to the rms width in the asymmetries of interest (driven by counting statistics) so that they do not reduce the statistical significance of the result and are averaged to zero quickly compared to the time it takes to measure the asymmetry to the desired accuracy. Possible false asymmetries due to spin-state correlated electronic pickup (additive asymmetry) and possible magnetic field-induced gain changes (multiplicative asymmetry) in the detector VPDs have previously been measured and are consistent with zero to within 5×10^{-9} [20].

The detector pair physics asymmetries as represented by Eq. (15) can then be combined in error weighted averages over the neutron time-of-flight spectrum to form a single asymmetry for each detector pair in the array, for a single eight-step sequence of beam pulses. If beam intensity levels are sufficiently stable over the measurement time these sequence asymmetries can be histogrammed for each pair. Typical run lengths were ~8.3 min and included 10,000 beam pulses or 1,250 eight-step sequences and the asymmetry measurements performed usually extended over several hundred runs.

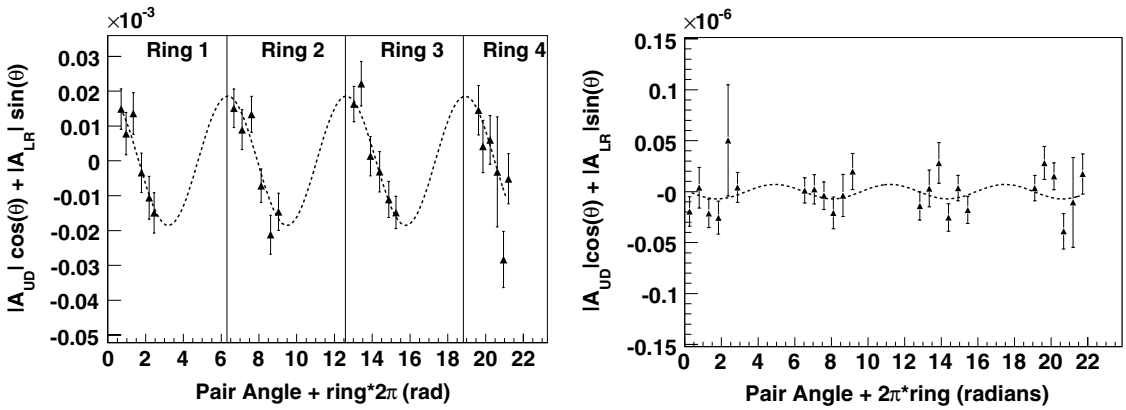

FIG. 5. (Left) CCl_4 asymmetries for each pair, plotted versus angle of the first detector in the pair with respect to the vertical. The total array asymmetry is extracted from the fit. (Right) Noise asymmetries.

TABLE IV. Up-down and left-right asymmetries for the target materials. Stated errors are statistical only. The rms widths are taken from histograms with single eight-step sequence asymmetries for a detector pair as individual entries.

	Asymmetries and rms width		
	Up-down	Left-right	rms width (typ.)
Al	$(-0.02 \pm 3) \times 10^{-7}$	$(-2 \pm 3) \times 10^{-7}$	1.2×10^{-3}
CCl_4	$(-19 \pm 2) \times 10^{-6}$	$(-1 \pm 2) \times 10^{-6}$	1.0×10^{-3}
B_4C	$(-1 \pm 2) \times 10^{-6}$	$(-5 \pm 3) \times 10^{-6}$	0.7×10^{-3}
Cu	$(-1 \pm 3) \times 10^{-6}$	$(0.3 \pm 3) \times 10^{-6}$	1.0×10^{-3}
In	$(-3 \pm 2) \times 10^{-6}$	$(3 \pm 3) \times 10^{-6}$	0.4×10^{-3}
Noise (add.)	$(2 \pm 5) \times 10^{-9}$	$(-7 \pm 5) \times 10^{-9}$	2.0×10^{-6}
Noise (mult.)	$(3 \pm 7) \times 10^{-9}$	$(-9 \pm 7) \times 10^{-9}$	0.2×10^{-3}
Beam · gain	N/A	N/A	1.0×10^{-5}

B. Results

The known parity-odd γ asymmetry in CCl_4 was used to verify that a nonzero asymmetry can be measured with our apparatus. The CCl_4 asymmetry was also used to verify the geometrical dependence of the pair asymmetries. For this purpose all 24 pair asymmetries, extracted from the histogrammed eight-step sequence asymmetries over all data obtained with that target, were multiplied by their mean geometry factors and plotted versus their corresponding mean angle, as shown in Fig. 5. The fit function used to extract the total array asymmetry is $A_{UD}\cos\theta + A_{LR}\sin\theta$.

In general, the up-down and left-right asymmetries must be extracted using the fit described above. Higher-order corrections to the fitting function used here (parity violating or not) are introduced by higher partial waves in the expansion of the initial and final two nucleon states representing more complicated scalar combinations between the neutron spin $\vec{s}_n$ and outgoing γ-ray momentum direction $\vec{k}_\gamma$. For the up-down asymmetry the angular distribution is obtained from initial and final two-nucleon states with components up to the P waves producing the $\vec{s}_n \cdot \vec{k}_\gamma$ correlation. The left-right asymmetry originates from the $\vec{s}_n \cdot (\vec{k}_\gamma \times \vec{k}_n)$ correlation. Parity-violating corrections from higher partial waves are negligible because they represent a second-order perturbation proportional to the weak coupling squared. The results of the asymmetry measurements are summarized in Table IV. Note that beam asymmetries are only produced if there are pulse-to-pulse fluctuations in the number of neutrons and only in combination with a difference in gain between a given detector pair. Neither beam fluctuations nor detector gain differences are correlated with the neutron spin and therefore the beam gain asymmetry contains no up-down or left-right dependence. Due to the sum over the eight-step sequence, the beam gain asymmetry is zero and its rms width is determined by the size of beam fluctuations. The additive and multiplicative noise asymmetries in Table IV are measured without a light signal from the detectors (electronic noise only) and with a light signal from light-emitting devices (LEDs) embedded in the detectors, respectively. The large rms width for the multiplicative noise asymmetry is a result of larger fluctuations with LEDs [20].

C. Errors

The final statistical errors stated in Table IV are taken from the distribution of sequence values $\sigma_\gamma^2/N = [E(A_\gamma^2) - E(A_\gamma)^2]/N$, with N histogrammed eight-step sequence asymmetries. Any nonrandom effect such as those introduced by the correction factors $|\langle G(t_i)\rangle|$, $\Delta_{\rm dep}(t_i)$, $P_n(t_i)$, $\Delta_{sf}(t_i)$ are treated as systematic errors. These enter as

$$\sigma_{\gamma,\rm Sys} = A_\gamma \sqrt{\left(\frac{\sigma_{P_n}}{P_n}\right)^2 + \left(\frac{\sigma_{sf}}{\Delta_{sf}}\right)^2 + \left(\frac{\sigma_G}{G}\right)^2 + \left(\frac{\sigma_{\rm dep}}{\Delta_{\rm dep}}\right)^2}$$

and are added in quadrature with the statistical error.

The errors on the beam polarization and spin flip efficiency were calculated to be 4 and 10%, respectively. The error on the geometry factor is estimated to be less than 1% from variations observed in the values when varying the step size in the Monte Carlo, simulating γ-ray interaction in the detectors. The error on the spin-flip scattering is estimated to be on the order of a few percent. Because the systematic errors are scaled by the asymmetry, their contribution to the overall error on the asymmetry is negligible compared to the statistical error, except for the case of the CCl_4 target, which has a large nonzero asymmetry. For CCl_4, the systematic error is $\simeq 2.3 \times 10^{-6}$. So the CCl_4 up-down physics asymmetry and its total error is $(-19 \pm 3) \times 10^{-6}$. A previous measurement of this asymmetry by this collaboration found $(-29.1 \pm 6.7) \times 10^{-6}$ [31]. M. Avenier and collaborators [10] found an up-down asymmetry for ^{35}Cl of $(-21.2 \pm 1.7) \times 10^{-6}$, whereas V. A. Vesna and collaborators found $(-27.8 \pm 4.9) \times 10^{-6}$ [11] (see also Ref. [32]).

V. CONCLUSION

The NPDGamma collaboration has searched for γ-ray asymmetries from polarized slow neutron capture on ^{27}Al, Cu, ^{115}In, and B_4C. The asymmetry measurements for these targets were consistent with zero at the few 10^{-7} level for ^{27}Al and at the few 10^{-6} level for Cu and ^{115}In. All asymmetries are consistent with zero within errors. The ^{35}Cl asymmetries obtained from the CCl_4 measurements are consistent with results from previous measurements. A statistical model, in combination with previous measurements of weak matrix

elements in compound nuclei, was used to estimate the expected rms size of the parity violating γ-ray asymmetries in ^{27}Al, Cu, and ^{115}In . Based on this model it is expected that nonzero measured asymmetries will be smaller than the estimated width 68.3% of the time. The upper bounds on the measured asymmetries are therefore consistent with the estimates obtained from these statistical calculations. Based on the inverse relationship between the single-particle level spacing and the size of the asymmetry, one would expect a large number of very small or essentially zero asymmetries when performing measurements for many larger nuclei, but one would also expect to find a small number of nuclei with enhanced asymmetries. We have already completed measurements in other nuclei, with higher precision, in the mass range $A > 50$ to further investigate the predictions of the statistical approach to parity violation in compound nuclei.

ACKNOWLEDGMENTS

The authors thank Mr. G. Peralta (LANL) for his technical support during this experiment, Mr. W. Fox (IUCF) and Mr. T. Ries (TRIUMF) for the mechanical design of the detector array and the construction of the stand, and Mr. M. Kusner of Saint-Gobain in Newbury, Ohio, for interactions during the manufacture and characterization of the CsI(Tl) crystals. We also thank TRIUMF for providing the personnel and infrastructure for the stand construction. This work was supported in part by the U.S. Department of Energy (Office of Energy Research, under contract W-7405-ENG-36), the National Science Foundation (grants PHY-0100348 and PHY-0457219), the NSF Major Research Instrumentation program (NSF-0116146), the Natural Sciences and Engineering Research Council of Canada, and the Japanese Grant-in-Aid for Scientific Research A12304014.

[1] S. S. M. Wong, *Nuclear Statistical Spectroscopy* (Oxford University Press, Oxford, 1986).
[2] C. E. Porter, *Statistical Theories of Spectra: Fluctuations* (Academic Press, New York, 1965).
[3] H. L. Harney, A. Richter, and H. A. Weidenmüller, Rev. Mod. Phys. **58**, 607 (1986).
[4] G. E. Mitchell, J. D. Bowman, and H. A. Weidenmüller, Rev. Mod. Phys. **71**, 445 (1999).
[5] G. E. Mitchell, J. D. Bowman, S. I. Penttilä, and E. I. Sharapov, Phys. Rep. **354**, 157 (2001).
[6] V. V. Flambaum and O. P. Sushkov, Nucl. Phys. **A435**, 352 (1985).
[7] V. V. Flambaum and G. F. Gribakin, Prog. Part. Nucl. Phys. **35**, 423 (1995).
[8] A. C. Hayes and L. Zanini, Phys. Rev. C **65**, 058501 (2002).
[9] V. E. Bunakov, V. P. Gudkov, S. G. Kadmensky, L. A. Lomachenkov, and V. I. Furman, Yad. Fiz. **40**, 188 (1984); Sov. J. Nucl. Phys. **40**, 119 (1984).
[10] M. Avenier *et al*., Nucl. Phys. **A436**, 83 (1985).
[11] V. A. Vesna *et al*., JETP Lett. **36**, 209 (1982).
[12] J. D. Bowman, L. Y. Lowie, G. E. Mitchell, E. I. Sharapov, and Y. F. Yen, Phys. Rev. C **53**, 285 (1996).
[13] E. G. Adelberger and W. C. Haxton, Annu. Rev. Nucl. Part. Sci. **35**, 501 (1985).
[14] T. von Egidy and D. Bucurescu, Phys. Rev. C **72**, 044311 (2005).
[15] W. Dilg, W. Schantl, and H. Vonach, Nucl. Phys. **A217**, 269 (1973).
[16] J. Kopecky and M. Uhl, in *Measurement, Calculation and Evaluation of Photon Production Data*, edited by C. Coceva, A. Mengoni, and A. Ventura (NEA/NCS/DOC, Bologna, 1994).
[17] C. M. McCullagh, M. L. Stelts, and R. E. Chrien, Phys. Rev. C **23**, 1394 (1981).
[18] S. F. Mughabghab, M. Divadeenam, and N. E. Holden, *Neutron Cross Sections Part A* (Z = 1–60) (Academic Press, New York, 1981).
[19] S. F. Mughabghab, M. Divadeenam, and N. E. Holden, *Neutron Cross Sections Part A* (Z = 61–100) (Academic Press, New York, 1984).
[20] M. T. Gericke *et al*., Nucl. Instrum. Methods A **540**, 328 (2005).
[21] W. S. Wilburn, J. D. Bowman, M. T. Gericke, and S. I. Penttilä, Nucl. Instrum. Methods A **540**, 180 (2005).
[22] P.-N. Seo *et al*., Nucl. Instrum. Methods A **517**, 285 (2004).
[23] T. E. Chupp, *et al*., Submitted to Nucl. Instrum. Methods (2006).
[24] T. Gentile *et al*., J. Res. Natl. Inst. Stand. Technol. **110**, 299 (2005).
[25] G. L. Jones *et al*., Nucl. Instrum. Methods A **440**, 772 (2000).
[26] P-N. Seo *et al*., to be submitted to Nucl. Instrum. Methods (2006).
[27] W. B. Davenport and W. L. Root, *An Introduction to the Theory of Random Signals and Noise* (John Wiley & Sons, New York, 1987).
[28] M. T. Gericke *et al*., J. Res. Natl. Inst. Stand. Technol. **110**, 215 (2005).
[29] A. Csoto, B. F. Gibson, and G. L. Payne, Phys. Rev. C **56**, 631 (1997).
[30] J. D. Bowman and J. C. VanderLeeden, Nucl. Instrum. Methods **85**, 19 (1970).
[31] G. S. Mitchell *et al*., Nucl. Instrum. Methods A **521**, 468 (2004).
[32] P. A. Krupchitskii *et al*., Phys. Part. Nucl. **25**, 6, 612 (1994).